iPSCs-derived mesenchymal stromal cells mitigate anxiety and neuroinflammation in aging female mice

Xiaoyue Wei[1,2,3,] †, Ruijie Li[1,2,] †, Xiangyu Li[1,2,] †, Boyan Wang[1,2], Jianyang Huang[1,2], Hanyiqi Mu[1,2], Qinmu Zhang[1,2], Ziyuan Zhang[1,2], Yifei Ru[1,2], Yinong Huang[2,4], Yuan Qiu[1,2], Yanchen Ye[5], Yuanyuan Feng[1], Shiyu Wang[1], Hui Chen[6], Chenju Yi[1,*], Jiancheng Wang[1,2,*]

1. Research Center, The Seventh Affiliated Hospital of Sun Yat-sen University, Shenzhen, 518107, China;
2. Center for Stem Cell Biology and Tissue Engineering, Key Laboratory for Stem Cells and Tissue Engineering, Ministry of Education, Sun Yat-Sen University, Guangzhou, 510080, China;
3. Zhongshan Ophthalmic Center, Sun Yat-Sen University, Guangzhou, 510060, China;
4. Department of Endocrinology, The First Affiliated Hospital of Sun Yat-Sen University, Guangzhou, 510080, China;
5. National-Guangdong Joint Engineering Laboratory for Diagnosis and Treatment of Vascular Diseases, The First Affiliated Hospital, Sun Yat-sen University, Guangzhou, 510080, China;
6. School of Life Sciences, Faculty of Science, University of Technology Sydney, Ultimo, NSW 2007, Australia.

† equal contribution

***Correspondence**

Associate Professor Chenju Yi, Scientific Research Center, The Seventh Affiliated Hospital of Sun Yat-Sen University, Shenzhen, Guangdong, China. E-mail: yichj@mail.sysu.edu.cn

Dr. Jiancheng Wang, Scientific Research Center, The Seventh Affiliated Hospital of Sun Yat-Sen University, Shenzhen, Guangdong, China. E-mail: wangjch38@mail.sysu.edu.cn

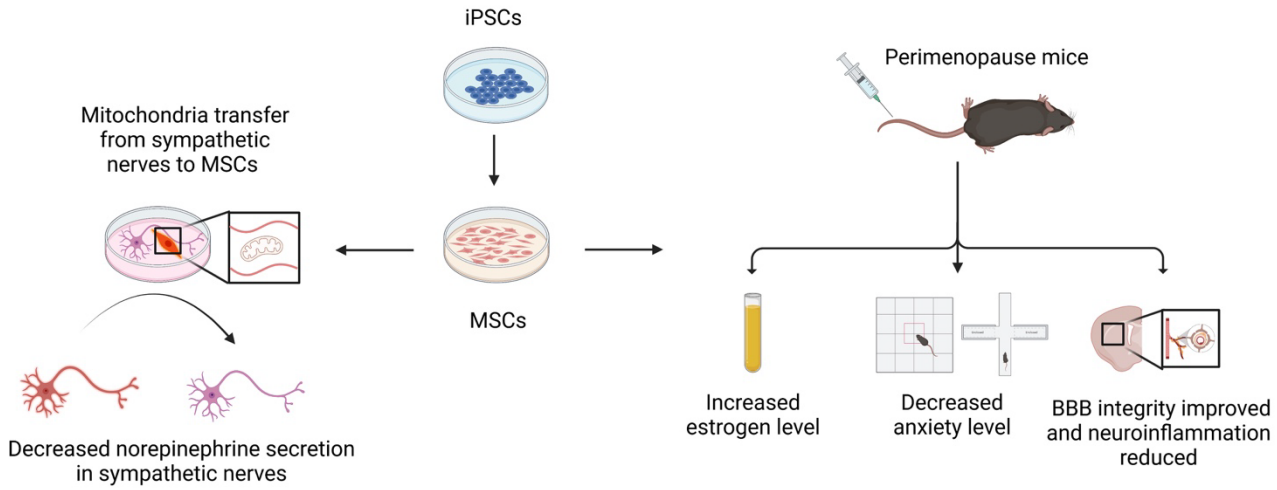

Abstract

Perimenopause is a natural transition to menopause, when hormone disturbance can result in both short-term mental disorders, such as anxiety, and long-term neuroinflammation due to blood-brain barrier (BBB) impairment, which may lead to more serious neurological disorders later on, such as dementia. Effective treatments may prevent both short-term and long-term neurological sequela, which formed the aim of this study. In aged female C57BL/6 mice (16-18 months of age), mesenchymal stromal cells (MSCs) differentiated from human-induced pluripotent stem cells (iPSCs), were administered via tail vein injection. Mice showed increased blood estrogen levels, alleviated anxiety and neuroinflammation, and improved BBB integrity. Interestingly, transplanted MSCs were located close to ovarian sympathetic nerves and decreased ovarian norepinephrine levels, which in turn increased ovarian estrogen secretion. Moreover, the administration of anastrozole, an inhibitor of estrogen synthesis, diminished the therapeutic effects of MSCs in vivo, suggesting the effect to be estrogen-dependent. *In vitro* study confirmed the impact of MSCs on sympathetic nerves via mitochondria exchange. In conclusion, iPSC-derived MSCs may provide a novel option to manage perimenopause-related hormonal dysregulation and neurological disorders during the female aging process.

Keywords: estrogen, cognition, blood-brain barrier, sympathetic nerve, mitochondria

Introduction

Perimenopause is a transition period during the female aging process [1], mainly caused by a drop in endogenous estrogen levels. Such hormone disturbance often results in perimenopausal neurological changes, including short-term increase in anxiety level and age-related blood-brain barrier (BBB) impairment which marks the initiation of long-term/permanent neurological dysfunctions [2]. Neuroinflammation due to impaired BBB protection against blood-borne neural toxins can increase the risk of neurodegenerative diseases, such as dementia and Alzheimer's disease [3]. Estrogen has been shown to exert neuroprotective effects by strengthening BBB integrity and exerting anti-inflammatory properties [4-6]. As a result, hormone replacement therapy is effective in improving both short-term perimenopausal anxiety and long-term neurological function[7]. However, hormone replacement therapy can also increase the risks of coronary vascular diseases and breast cancer, limiting the application of such a treatment. Exogenous hormone at a standard dose may also disturb the natural rhythm of estrogen and other sex hormone secretion [8,9]. Therefore, novel approaches are needed to improve life quality during perimenopause by improving endogenous estrogen production according to the needs of the individuals.

Traditionally, the hypothalamic-pituitary-ovarian axis is believed to be the primary regulator of estrogen secretion. However, recent research has focused on direct sympathetic control within the ovary as another crucial neuroendocrine mechanism underlying estrogen-related physiological activity [10]. Optimal sympathetic stimulation is essential for ovarian follicle growth and estrogen secretion [11]. Hyperactivity of ovarian sympathetic tone has been found during aging [2], which impairs follicular development resulting in reduced estrogen secretion and ovarian degeneration [12,13]. Increased ovarian sympathetic activities are also the feature underlying dysregulated estrogen secretion in polycystic ovarian syndrome [14,15]. Indeed, mental health disorders, including anxiety, are common among patients with polycystic ovarian syndrome[16]. Given the close link between sex hormone deregulation and cognitive impairment during the perimenopausal period, therapeutic strategies that can improve both endocrine functions of the ovary and alleviate neuronal dysfunction are appealing.

Mesenchymal stromal cells (MSCs) are self-renewable cells that possess osteogenic, chondrogenic, and adipogenic progeny [17-19]. They are one of the most commonly studied stem cells for cell-based therapies. Due to the ability to secrete neurotrophic and antioxidative factors, MSCs have been proposed in anti-aging [20] and neurodegenerative disease treatments to improve neurological function, such as Parkinson's disease and Alzheimer's disease [21,22]. The primary MSCs from human donors (bone marrow-derived) are heterogeneous, determined by their origin (biological niche) or the conditions of the donors (eg. age, sex, disease status) [23,24]. Additionally, primary MSCs only have limited passages. Such properties of primary MSCs have limited their clinical application and pose a significant manufacturing challenge. Human induced pluripotent stem cells (iPSCs) can differentiate into homogenous MSCs, which can overcome the above limitations of primary MSCs in future clinical trials. Therefore, this study aimed to investigate whether iPSCs-derived MSCs can improve

neuroendocrine disorders in aged female mice. Here, MSC transplantation increased the circulating estrogen levels in aged female mice, accompanied by alleviated anxiety-like behaviors, BBB integrity and neuroinflammation. Interestingly, transplanted MSCs were localized near ovarian sympathetic nerve fibers and inhibited ovarian sympathetic activities. In vitro study suggests the mitochondria exchange between sympathetic neurons and MSCs is vital in the interactions between MSCs and sympathetic nerves.

Materials and Methods

Animal experiments

This study was approved by the Ethical Committee of Sun Yat-Sen University (2021001559) and performed according to the guide for the care and use of laboratory animals. Female C57BL/6 mice aged between 2-3 months (young) and 16-18 months (aged) were obtained from the Guangdong Medical Laboratory Animal Center (Guangzhou, China) and housed under a 12 h light/dark cycle (lights on at 7:00, lights off at 19:00) and 22 ± 2°C, with *ad libitum* access to food and water. Young mice were used as the healthy control. The aged mice were randomly assigned to 3 groups: Control, MSC treatment, and ANS (anastrozole) + MSC.

Prior to the behavioral tests, mice were habituated to the apparatus for 3 days. All experiments were performed during the light cycle. Locomotion and anxiety-like behaviors were assessed by the open-field test. Mice were placed in a 45 x 45 cm arena and tracked by TopScan software (CleverSys Inc, VA, USA). Anxiety-like behaviors were examined by the time spent in the central zone. Locomotion was evaluated by the total distance travelled. An elevated plus maze was illuminated by 60Lx in the open arms and 10–20Lx in the close arms. Mice were habituated with 10–20Lx light for 1h before the test. During the test, a mouse was introduced to the closed arm and allowed to explore the maze freely for 5min and filmed. Videos were analyzed by an experimenter blinded to the group codes. Anxiety-like behaviors were reported as the percentage of time spent in the open arm during the 5 minutes.

MSC treatment

The lentiviral vectors were designated as pLV/puro-EF1a-dtomato, as previously described [25]. Lentiviral particles were harvested from 293FT cells. Briefly, when 293FT cells reached 70% confluent, transiently transfecting 293FT with lentiviral vectors together with packaging vectors pMD2-VSVG and pPAX2 by using Fugene 6 (Promega, WI, USA). Supernatant was collected 48 h after transfection. MSCs (passage 3) were transfected with tdTomato vector to trace in vivo. Three days after transduction, MSCs were sorted using fluorescence-activated cell sorting (FACS, Influx, Becton Dickinson, CA, USA).

For MSC administration, $1x10^6$ cells (passages 4-8) were suspended in 0.1 ml PBS and administered via the caudal vein ten days prior to the behavioral tests. To determine whether the effect of MSC is estrogen-dependent, MSC treated group was also given anastrozole (0.2mg/kg/day, Selleck in water, ZD-1033, oral administration) for 10 days, which is an inhibitor of aromatase enzyme that can

effectively reduce circulating estrogen levels [26].

Cell culture

The human iPSCs line was established as previously described [27]. The cells were cultured on Matrigel (BD Bioscience, CA, USA)-coated plates in mTeSR1 medium (Stemcell Technologies, AB, Canada). The cells were passaged every 4-5 days using the StemPro Accutase Cell Dissociation Reagent (Thermo Fisher, CA, USA).

To differentiate iPSCs into neuromesodermal progenitors, iPSCs were dissociated into single cells by incubation with Accutase (Thermo Fisher, CA, USA) at 37℃ for 2-3 minutes and cultured on Matrigel-coated plates in mTeSR1 medium containing 10 μM Y27632 (Sigma-Aldrich, MO, USA) for 24 hours. Then, these cells were cultured in the Essential 6 medium supplemented with basic fibroblast growth factor (20 ng/ml, Thermo Fisher, CA, USA), TGFβ1 (2-5 ng/ml, Peprotech, NJ, USA), and CHIR99021 (10 μM, Stemgent, MA, USA) for 2-5 days. For MSCs differentiation, neuromesodermal progenitors were cultured in animal component-free (ACF) and serum-free medium (MesenCult™-ACF Plus Medium; Stemcell Technologies, VAN, CAN) for 2-3 weeks. The differentiated cells were maintained in MesenCult™-ACF Plus Medium.

For sympathetic neuron differentiation, CHIR99021 (1.5 μM)-treated day 3 cell aggregates were cultured in Essential 6 medium supplemented with FGF2 (20 ng/mL), retinoic acid (1μM, Sigma-Aldrich, MO, USA) and Purumorphamine (1μM, Sigma-Aldrich, CA, USA). At day 10, the cells were dissociated into single cells to isolate $CD49d^{-}eGFP^{+}$ cells by FACS. $CD49d^{-}eGFP^{+}$ cells were cultured on Growth Factor Reduced Matrigel Matrix-coated culture plates with Neurobasal Medium (Gibco, CA, USA), N2 and B27 supplement (Gibco, CA, USA), Compound E (100 nM, Gibco, CA, USA), neurotrophic factors BDNF and GDNF (both 10 ng/mL, Gibco, CA, USA). Y27632 (20 μM, Sigma-Aldrich, MO, USA) was added in the first two days. The cells were passaged once at 7-10 [28].

To examine the ability to differentiate into osteogenic, adipogenic, and chondrogenic neurons, iPSCs-derived MSCs were cultured in the relevant differentiation medium for 2 or 3 weeks and analyzed with alizarin red, oil red O, and toluidine blue staining as previously reported [29].

iPSCs-derived MSCs and sympathetic neurons (iPSCs-SN) were co-cultured (10:1 ratio, total 11,000 cells) on a scaffold made from collagen I in a mixture of MSCs medium and sympathetic neurons medium described above (1:1 ratio, supplied with Cytochalasin D (1μM, Sigma-Aldrich, MO, USA)) at 37°C (21% O_2 and 5% CO_2) for 48h before experiments. A 12-well Transwell system (pore size 0.4 μm; Corning Incorporated, NY, USA) was used to prevent direct contact between two cell types. Sympathetic neurons were seeded in the lower layers (10^3 cells/well), while iPSCs-derived MSCs were seeded in the upper layers (10^4 cells/well). The same MSCs medium and sympathetic neurons medium mixture were used for 48h before experiments.

For the mitochondria transfer experiment, MSCs were transfected with GFP lentivirus（Roche, BS,

Switzerland） as previously described[30]. The medium was changed 12h after transfection. Three days after transfection, GFP-labeled MSCs were purified by FACS (Influx, Becton Dickinson, CA, USA). iPSCs-SNs were stained with MitoTracker Red according to the manufacturer's instructions (Invitrogen, CA, USA). Briefly, a pre-warmed staining solution containing 100 nM MitoTracker was added to iPSCs-SNs for 30min. Then, iPSCs-SNs were washed with phosphate-buffered saline (PBS) and GFP^+ MSCs were added. iPSCs-SNs and MSCs were directly co-cultured in a mixture of MSCs medium and sympathetic neurons medium described above (1:1 ratio) for 48h.

Immunofluorescence staining

Cells were fixed with 4% Paraformaldehyde at room temperature for 20 min and rinsed three times with PBS. Cells were permeabilized with 0.3% Triton X-100 and incubated with primary antibody or isotype control containing 5% BSA or goat serum overnight at 4°C, followed by relevant secondary antibodies for 1h at room temperature (antibody details in Supplementary Table 1). Samples were then counterstained with 4′,6-diamidino-2-phenylindole (DAPI, Sigma Aldrich, MO, USA). Sectioned frozen brain samples (100 μm) were used for immunostaining. Tight junction protein (ZO-1) was co-stained in the isolectin B4 (IB4) positive endothelial cell. Immune cells in the brain were stained with Ly6g or CD3. All images were taken by Dragonfly highspeed confocal microscopy (ANDOR, Oxford Instruments, OXF, UK). Image J 1.52a (NIH, USA) was used to analyze the images.

Flow cytometry

MSCs were incubated for 30min with the appropriate antibody such as CD29, CD44, CD73, CD90, CD34, CD45 (Invitrogen, CA, USA) in the dark at 4°C, and then analyzed by flow cytometry using Influx (BD) or Gallios (Beckman Coulter, CA, USA) flow cytometers. Each analysis was performed on three separate cell preparations. The data were analyzed by FlowJo software (Version 7.6.1, Treestar, USA)

Bioassays

Serum estrogen was measured by a commercial ELISA kit (CusaBio, DE, USA) following the manufacture’s instructions. Briefly, serum and HRP-conjugated test solution were incubated for 1 hour at 37ºC, followed by incubation with Substrate A and B for 15 minutes at 37°C. The color change was measured using a microplate reader at 450nm ( ). Norepinephrine secretion in culture media was measured by commercially available ELISA kits according to the manufacturer's instructions (MAISHA, Shanghai, China).

Total ROS and mitochondrial ROS were stained using the fluorescent probes, CellROX Deep Red and MitoSOX (Molecular Probes, Thermo Fisher, CA, USA), respectively, and analyzed by flow cytometry and confocal microscopy.

Quantitative real-time PCR

Total mRNA from the cells and tissues was extracted using the TRIzol Reagent (Invitrogen, CA,

USA), and reverse transcription was performed using a QuantiTect Reverse Transcription kit (Qiagen, DE USA) according to the manufacturer's instructions. Quantitative real-time PCR analysis was performed using a DyNAmo ColorFlash SYBR Green qPCR kit (Thermo Fisher, CA, USA) and the LightCycler 480 Detection System (Roche, BS, Switzerland). Glyceraldehyde-3-phosphate dehydrogenase (GAPDH) was used as the housekeeping gene, and target gene expression was calculated as fold change using the $2^{-\Delta\Delta Ct}$ method. Primer details are provided in Supplementary Table 1.

Statistical analysis

Data are reported as mean ± SEM and analyzed using unpaired Student's t test, one-way ANOVA, or X2 test where applicable (GraphPad Prism 7, GraphPad, CA, USA). Six mice were used for each group. Three independent experimental repeats were used for all *in vitro* studies. $P < 0.05$ was considered statistically significant.

Results

Cell phenotype confirmation

The pluripotency of iPSCs was confirmed by the positive immunostaining of pluripotency markers, including Nanog, SOX2 and Oct4 (Figure S1a). iPSCs derived MSCs showed high levels of MSC-specific markers, including CD29, CD44, CD73, and CD90. In contrast, there was no staining of markers for immune cells (CD45, CD34) and endothelial cells (CD31, Figure S1b). Tri-lineage differentiation showed that iPSCs-derived MSCs can be differentiated into three cell types, ie. adipocytes, osteoblasts, and chondrocytes (Figure S1b).

MSC treatment alleviated anxiety-like behaviors in the aged mice.

After the treatment of iPSC-derived MSCs, the serum estrogen level was increased in the aged mice, suggesting that MSC therapy restored ovarian estrogen endocrine function (Figure 1a). Reduced estrogen level is closely associated with perimenopausal anxiety [2]. Indeed, compared with the young mice, aged mice spent less time in the central zone and less active in the open field (Figure 1b-d), as well as less time in the open arms of the elevated plus maze (Figure 1e, f). The performance in both tests turned to the young mice level in aged mice treated with MSCs (Figure 1b-f), suggesting ameliorated anxiety and locomotion.

MSCs migrated to the ovaries in close proximity to the sympathetic nerves in aged mice

To locate transplanted iPSC-derived MSCs (Figure 2a) *in vivo*, MSCs were transfected with tdTomato lentivirus in red (Figure 2b). Interestingly, MSCs were found nearby the sympathetic nerve of the ovaries (Figure 2c). The ovarian sympathetic nerves are close to ovarian blood vessels (Figure S2a), via which MSCs gained access to ovarian sympathetic nerves. Both plasma and ovarian norepinephrine concentrations were increased in aged mice compared with the young mice ($P<0.05$), which were inhibited by MSCs in aged mice ($P<0.05$, Aged vs Aged + MSC. Figure 2d-e). Thus,

MSC therapy suppressed ovarian sympathetic hyperactivity to increase estrogen secretion.

MSCs inhibited norepinephrine secretion from the sympathetic nerves *in vitro*

To investigate how MSCs regulate ovarian sympathetic nerve activity, iPSC-SNs were generated (Figure 3a) and co-cultured with iPSC-derived MSCs. iPSC-SNs were tyrosine hydroxylase positive and spindle-shaped (Figure 3b), and capable of secreting norepinephrine (Figure 3c). In the direct co-culture system, norepinephrine concentration in the culture media was inhibited by the presence of MSCs ($P<0.05$), but not in the transwell co-culture system (Figure 3c), suggesting the need for direct contact between these two cell types.

The antioxidative ability of MSCs has been well documented in the direct co-culture system, where the total ROS and mitochondrial ROS levels in the iPSC-SNs were significantly decreased in the presence of MSCs (Figure 3d,e), suggesting a positive correlation between mitochondrial ROS production and sympathetic nervous activity.

Mitochondria transfer between sympathetic neurons and MSCs to suppress oxidative stress.

After co-cultured with MSCs, mitochondria in the iPSC-SNs labeled with MitoTracker Red were observed in the cytoplasm of MSCs (Figure 4a), which suggests that MSCs received mitochondria from iPSC-SNs. Interestingly, reverse transfer from MSCs to iPSCs-SNs was not observed (data not shown). Therefore, iPSC-SNs may signal MSCs to exert antioxidant effects by transferring stressed mitochondria to MSCs.

Intercellular mitochondria transfer can be mediated by tunneling nanotubes (TNTs) [31,32]. Here, positive TNT staining was found in the mitochondria transferred from iPSC-SNs to MSCs (Figure 4b). We then used actin polymerization inhibitor cytochalasin D to block TNT formation in the co-cultured cells. Mitochondria transfer from iPSC-SNs to MSCs was significantly reduced by cytochalasin D (Figure 4c). As a result, MSCs failed to inhibit norepinephrine secretion (Figure 4d) and ROS levels in the iPSC-SNs (Figure 4e-f), suggesting that mitochondria transfer from iPSC-SNs to MSCs is an important signal cue in MSC regulation of sympathetic tone. Among all the adhesion molecules measured here, N-Cadherin expression was significantly increased after co-culture, suggesting its involvement in the adhesion between MSCs and iPSC-SNs (Figure 4g).

Anastrozole blocked the therapeutic effects of MSCs.

As an aromatase inhibitor, anastrozole can inhibit estrogen production (Figure S3a). Anastrozole administration in MSC-treated aged mice reduced their activity and time spent in the central zone during the open-field test (Figure 5a-c) and the time spent in the open arms of the elevated plus maze (Figure 5d-e). These results suggest that estrogen is the key mechanism by which MSCs attenuate anxiety and promote locomotion in aged mice.

MSC treatment improved BBB integrity and reduced neuroinflammation.

Compared with the young mice, endothelial tight junction protein ZO-1 was reduced by half in aged

mice (Figure 6a, e), accompanied by significantly increased albumin leakage from the vessels (Figure 6b, f). These results suggested disrupted BBB in aged mice, which was closely associated with increased infiltration of proinflammatory immune cells in the brain (Figure 6c, g, h) and microglial activation (Figure 6d, i). While MSC treatment in aged mice improved BBB integrity and ameliorated inflammatory responses in the brain, anastrozole nearly diminished such therapeutic effects of MSC (Figure 6). These results suggest that optimal endogenous estrogen production may play a vital role in preventing aging-related anxiety and BBB impairment.

Discussion

The major finding of this study is the ability of MSCs to reduce anxiety and improve BBB integrity and related neuroinflammation in aged female mice, by restoring the estrogen secretion function of the ageing ovaries. This discovery suggests a new option for managing neuroendocrine disorders and related complications, especially neurocognitive dysfunctions, among perimenopausal women.

In this study, restored ovarian estrogen secretion is the key to MSC transplantation-induced improvement in anxiety and neuroinflammation of old female mice. The regulation of local sympathetic tone is suggested to be the underlying cause. Increased ovarian sympathetic tone contributes to an adverse ovarian microenvironment in aging and causes deterioration of ovarian endocrine function [33]; while reduced estrogen level is closely associated with perimenopausal anxiety [2]. Here, the exogenous MSCs co-localized with the ovarian sympathetic nerve fibers, which resulted in a decrease in ovarian norepinephrine levels. This suggests that ovarian sympathetic activity was inhibited by MSC therapy, whereas enhanced ovarian sympathetic activity is a major cause of reduced estrogen production during aging.

The co-culture system allows us to have an insight into how MSC suppress sympathetic tone in the ovary. With direct contact with MSCs, oxidative stress in the sympathetic neurons was significantly reduced. MSCs have been shown to secrete antioxidants [21,22], which may contribute to reduced ROS in the adjacent sympathetic neurons. From the transwell system, it is clear that close contact between these two cell types is needed. Further investigation showed mitochondria transfer between the cells is a vital signal message to the MSCs to exert antioxidative effects and reduce norepinephrine secretion in the sympathetic neurons. Mitochondria transfer is one of the mechanisms of cell-to-cell communication. It has been shown that mitochondrial transfer can reduce cellular stress [34,35] and restore the mitochondrial function in recipient cells [36]. For example, after a stroke, astrocytes receive nonfunctional mitochondria from damaged neurons for disposal while transferring functional mitochondria to the injured neurons for recovery [37,38]. In this study, we also showed that the mitochondria transfer between MSCs and sympathetic nerves relies on TNT formation. TNTs are nanotubular structures from the outgrowth of filopodia-like cell membrane protrusions that connect with the target cell. It is mainly composed of F-actin and transport proteins that facilitate the active transport of cargo, e.g. mitochondria [39]. In addition, the adhesion molecule N-Cadherin is also the key

to the connection between sympathetic neurons and MSCs. Nevertheless, the interruption of TNT formation also diminished the effect of MSCs on decreasing ROS levels in the sympathetic neurons. It has been shown that oxidative stress can increase norepinephrine secretion[40]. Therefore, the antioxidant effect may be vital to inhibiting norepinephrine secretion by MSCs.

Estrogen can directly modulate anxiety behaviors [41]. Three estrogen receptors, ER□, ER□ and G-protein-coupled estrogen receptors, are found in neurons that control cognitive behaviors and mood in the brain [42]. Among them, ER□ plays an important role in anxiolytic-like effects in the central nervous system [43], through the hypothalamus-pituitary-adrenal axis and the serotonergic nervous system in the striatum [44]. Reduced estrogen secretion can decrease the number of serotonergic neurons in the brain [45]. Here, MSC treatment reduced anxiety and restored locomotor activities in aged mice, which largely depends on the blood estrogen levels in those mice. Future studies can examine the serotonergic nervous system, which is beyond the scope of this study.

MSCs have been trialed in neurodegenerative diseases to improve neurological function [21,22]. Here, the improved BBB function may also play a key role in improved cognitive function in the aged mice. BBB prevent neurotoxic substances in circulation from entering brain tissue, dependent on the normal function of tight junction proteins, such as ZO-1. BBB breakdown is common in aging patients, resulting in vascular leakage, inflammatory cell infiltration from the blood, and neuronal damage, which plays a crucial role in neurodegeneration and cognitive decline [46]. Here, MSCs treatment restored tight junction protein levels in the aging brain, reducing the infiltration of circulating inflammatory cells. In addition, estrogen has anti-inflammatory and immunomodulatory capacity [6]. Previous studies have suggested that estrogen can help maintain BBB integrity and limit inflammatory cell infiltration into the brain [6,47]. Indeed, in this study, the concurrent increase in blood estrogen suppressed the inflammatory response in the aging brain. Therefore, MSC therapy may improve aging brain health and cognitive function in an estrogen-dependent manner. Future studies can titrate the protocol of MSCs treatment, such as frequency, alternative routes, and different dosages.

Conclusions

MSC transplantation improved estrogen secretion and alleviated aging-related anxiety by improving BBB function and neuroinflammation in aged female mice. Therefore, MSC has the potential to be an effective cell therapeutic strategy for managing perimenopasual neuroendocrine disorders.

Abbreviations

MSC: mesenchymal stromal cell; BBB: blood-brain barrier; iPSCs: induced pluripotent stem cells; FACS: fluorescence-activated cell sorting; ACF: animal component-free; DAPI: 4′,6-diamidino-2-phenylindole; IB4: isolectin B4; ANS: anastrozole; PFA: Paraformaldehyde; PBS: phosphate-buffered saline; BSA: bovine serum albumin; ANOVA: One-way analysis of variance; iPSC-SNs: iPSC-derived sympathetic neurons; ROS: reactive oxygen species; TNTs: tunneling nanotubes.

Authors' contributions: X.W., R.L. and X.L. designed and performed the experiments. J.H., H.M., Y.Y., Z.Z., H.C. and Q.Z. wrote the manuscript. B.W., Y.R., Y.F. and S.Y. performed the statistical

analysis. J.W. and Y.H. obtained the funding support. C.Y. and Y.Q. coordinated the study. All authors read and approved the final manuscript.

Funding: This work was supported by **grants from** National Natural Science Foundation of China to Y.H. (No. 82101367) and J.W. (No.32170799 and No.81971372)

Institutional Review Board Statement: All animal experiments were approved by the Animal Ethics and Care Committee of Sun Yat-Sen University.

Informed Consent Statement: Not applicable.

Data Availability Statement: All the data are included in the manuscript.

Conflicts of Interest: The authors report no conflict of interest.

Reference:

1 Arlt, W. & Hewison, M. Hormones and immune function: implications of aging. *Aging cell* **3**, 209-216, doi:10.1111/j.1474-9728.2004.00109.x (2004).

2 Brinton, R. D., Yao, J., Yin, F., Mack, W. J. & Cadenas, E. Perimenopause as a neurological transition state. *Nature reviews. Endocrinology* **11**, 393-405, doi:10.1038/nrendo.2015.82 (2015).

3 Calsolaro, V. & Edison, P. Neuroinflammation in Alzheimer's disease: Current evidence and future directions. *Alzheimer's & dementia : the journal of the Alzheimer's Association* **12**, 719-732, doi:10.1016/j.jalz.2016.02.010 (2016).

4 Bromberger, J. T. & Kravitz, H. M. Mood and menopause: findings from the Study of Women's Health Across the Nation (SWAN) over 10 years. *Obstet Gynecol Clin North Am* **38**, 609-625, doi:10.1016/j.ogc.2011.05.011 (2011).

5 Xu, Y. *et al.* NLRP3 inflammasome activation mediates estrogen deficiency-induced depression- and anxiety-like behavior and hippocampal inflammation in mice. *Brain Behav Immun* **56**, 175-186, doi:10.1016/j.bbi.2016.02.022 (2016).

6 Maggioli, E. *et al.* Estrogen protects the blood-brain barrier from inflammation-induced disruption and increased lymphocyte trafficking. *Brain Behav Immun* **51**, 212-222, doi:10.1016/j.bbi.2015.08.020 (2016).

7 Paciuc, J. Hormone Therapy in Menopause. *Adv Exp Med Biol* **1242**, 89-120, doi:10.1007/978-3-030-38474-6_6 (2020).

8 Demetrio, F. N. *et al.* Effect of estrogen replacement therapy on symptoms of depression and anxiety in non-depressive menopausal women: a randomized double-blind, controlled study. *Arch Womens Ment Health* **14**, 479-486, doi:10.1007/s00737-011-0241-3 (2011).

9 Gleason, C. E. *et al.* Effects of Hormone Therapy on Cognition and Mood in Recently Postmenopausal Women: Findings from the Randomized, Controlled KEEPS-Cognitive and Affective Study. *PLoS Med* **12**, e1001833; discussion e1001833, doi:10.1371/journal.pmed.1001833 (2015).

10 Uchida, S. Sympathetic regulation of estradiol secretion from the ovary. *Auton Neurosci* **187**, 27-35, doi:10.1016/j.autneu.2014.10.023 (2015).

11 Mayerhofer, A., Dissen, G. A., Costa, M. E. & Ojeda, S. R. A role for neurotransmitters in

early follicular development: induction of functional follicle-stimulating hormone receptors in newly formed follicles of the rat ovary. *Endocrinology* **138**, 3320-3329, doi:10.1210/endo.138.8.5335 (1997).

12 Cruz, G., Fernandois, D. & Paredes, A. H. Ovarian function and reproductive senescence in the rat: role of ovarian sympathetic innervation. *Reproduction (Cambridge, England)* **153**, R59-r68, doi:10.1530/rep-16-0117 (2017).

13 Fernandois, D., Cruz, G., Na, E. K., Lara, H. E. & Paredes, A. H. Kisspeptin level in the aging ovary is regulated by the sympathetic nervous system. *The Journal of endocrinology* **232**, 97-105, doi:10.1530/joe-16-0181 (2017).

14 Shorakae, S. *et al.* Inter-related effects of insulin resistance, hyperandrogenism, sympathetic dysfunction and chronic inflammation in PCOS. *Clinical endocrinology* **89**, 628-633, doi:10.1111/cen.13808 (2018).

15 Lara, H. E. *et al.* Changes in sympathetic nerve activity of the mammalian ovary during a normal estrous cycle and in polycystic ovary syndrome: Studies on norepinephrine release. *Microscopy research and technique* **59**, 495-502, doi:10.1002/jemt.10229 (2002).

16 Himelein, M. J. & Thatcher, S. S. Polycystic ovary syndrome and mental health: A review. *Obstet Gynecol Surv* **61**, 723-732, doi:10.1097/01.ogx.0000243772.33357.84 (2006).

17 Galipeau, J. & Sensebe, L. Mesenchymal Stromal Cells: Clinical Challenges and Therapeutic Opportunities. *Cell Stem Cell* **22**, 824-833, doi:10.1016/j.stem.2018.05.004 (2018).

18 Zhang, W. *et al.* Aging stem cells. A Werner syndrome stem cell model unveils heterochromatin alterations as a driver of human aging. *Science* **348**, 1160-1163, doi:10.1126/science.aaa1356 (2015).

19 Klimczak, A. Mesenchymal Stem/Progenitor Cells and Their Derivates in Tissue Regeneration. **23**, 6652 (2022).

20 Phinney, D. G. & Pittenger, M. F. Concise Review: MSC-Derived Exosomes for Cell-Free Therapy. *Stem Cells* **35**, 851-858, doi:10.1002/stem.2575 (2017).

21 Kuo, S. C. *et al.* Mesenchymal stem cell-conditioned medium attenuates the retinal pathology in amyloid-β-induced rat model of Alzheimer's disease: Underlying mechanisms. *Aging cell* **20**, e13340, doi:10.1111/acel.13340 (2021).

22 Staff, N. P., Jones, D. T. & Singer, W. Mesenchymal Stromal Cell Therapies for Neurodegenerative Diseases. *Mayo Clinic proceedings* **94**, 892-905, doi:10.1016/j.mayocp.2019.01.001 (2019).

23 Wang, Z. *et al.* Single-cell transcriptome atlas of human mesenchymal stem cells exploring cellular heterogeneity. *Clinical and translational medicine* **11**, e650, doi:10.1002/ctm2.650 (2021).

24 Costa, L. A. *et al.* Functional heterogeneity of mesenchymal stem cells from natural niches to culture conditions: implications for further clinical uses. *Cell Mol Life Sci* **78**, 447-467, doi:10.1007/s00018-020-03600-0 (2021).

25 Huang, Y. *et al.* Targeted homing of CCR2-overexpressing mesenchymal stromal cells to ischemic brain enhances post-stroke recovery partially through PRDX4-mediated blood-brain barrier preservation. *Theranostics* **8**, 5929-5944, doi:10.7150/thno.28029 (2018).

26 Nelson, L. R. & Bulun, S. E. Estrogen production and action. *J Am Acad Dermatol* **45**, S116-124, doi:10.1067/mjd.2001.117432 (2001).

27 Li, W. *et al.* Characterization and transplantation of enteric neural crest cells from human induced pluripotent stem cells. *Molecular psychiatry* **23**, 499-508, doi:10.1038/mp.2016.191

(2018).
28 Kirino, K., Nakahata, T., Taguchi, T. & Saito, M. K. Efficient derivation of sympathetic neurons from human pluripotent stem cells with a defined condition. *Sci Rep* **8**, 12865, doi:10.1038/s41598-018-31256-1 (2018).
29 Yan, X. *et al.* Dispersible and Dissolvable Porous Microcarrier Tablets Enable Efficient Large-Scale Human Mesenchymal Stem Cell Expansion. *Tissue Eng Part C Methods* **26**, 263-275, doi:10.1089/ten.TEC.2020.0039 (2020).
30 Sang, J. F. *et al.* Combined mesenchymal stem cell transplantation and interleukin-1 receptor antagonism after partial hepatectomy. *World J Gastroenterol* **22**, 4120-4135, doi:10.3748/wjg.v22.i16.4120 (2016).
31 Fan, X. L., Zhang, Y., Li, X. & Fu, Q. L. Mechanisms underlying the protective effects of mesenchymal stem cell-based therapy. *Cell Mol Life Sci* **77**, 2771-2794, doi:10.1007/s00018-020-03454-6 (2020).
32 Spees, J. L., Lee, R. H. & Gregory, C. A. Mechanisms of mesenchymal stem/stromal cell function. *Stem Cell Res Ther* **7**, 125, doi:10.1186/s13287-016-0363-7 (2016).
33 Hale, G. E., Robertson, D. M. & Burger, H. G. The perimenopausal woman: endocrinology and management. *J Steroid Biochem Mol Biol* **142**, 121-131, doi:10.1016/j.jsbmb.2013.08.015 (2014).
34 Islam, M. N. *et al.* Mitochondrial transfer from bone-marrow-derived stromal cells to pulmonary alveoli protects against acute lung injury. *Nat Med* **18**, 759-765, doi:10.1038/nm.2736 (2012).
35 Lin, H. Y. *et al.* Mitochondrial transfer from Wharton's jelly-derived mesenchymal stem cells to mitochondria-defective cells recaptures impaired mitochondrial function. *Mitochondrion* **22**, 31-44, doi:10.1016/j.mito.2015.02.006 (2015).
36 Li, X. *et al.* Mitochondrial transfer of induced pluripotent stem cell-derived mesenchymal stem cells to airway epithelial cells attenuates cigarette smoke-induced damage. *Am J Respir Cell Mol Biol* **51**, 455-465, doi:10.1165/rcmb.2013-0529OC (2014).
37 Hayakawa, K. *et al.* Transfer of mitochondria from astrocytes to neurons after stroke. *Nature* **535**, 551-555, doi:10.1038/nature18928 (2016).
38 Davis, C. H. *et al.* Transcellular degradation of axonal mitochondria. *Proc Natl Acad Sci U S A* **111**, 9633-9638, doi:10.1073/pnas.1404651111 (2014).
39 Ahmad, T. *et al.* Miro1 regulates intercellular mitochondrial transport & enhances mesenchymal stem cell rescue efficacy. *EMBO J* **33**, 994-1010, doi:10.1002/embj.201386030 (2014).
40 Peixoto-Neves, D., Soni, H. & Adebiyi, A. Oxidant-induced increase in norepinephrine secretion from PC12 cells is dependent on TRPM8 channel-mediated intracellular calcium elevation. *Biochem Biophys Res Commun* **506**, 709-715, doi:10.1016/j.bbrc.2018.10.120 (2018).
41 Donner, N. & Handa, R. J. Estrogen receptor beta regulates the expression of tryptophan-hydroxylase 2 mRNA within serotonergic neurons of the rat dorsal raphe nuclei. *Neuroscience* **163**, 705-718, doi:10.1016/j.neuroscience.2009.06.046 (2009).
42 Revankar, C. M., Cimino, D. F., Sklar, L. A., Arterburn, J. B. & Prossnitz, E. R. A transmembrane intracellular estrogen receptor mediates rapid cell signaling. *Science* **307**, 1625-1630, doi:10.1126/science.1106943 (2005).
43 Burris, T. P. *et al.* Nuclear receptors and their selective pharmacologic modulators. *Pharmacol*

Rev **65**, 710-778, doi:10.1124/pr.112.006833 (2013).

44 Herman, J. P. & Cullinan, W. E. Neurocircuitry of stress: central control of the hypothalamo-pituitary-adrenocortical axis. *Trends Neurosci* **20**, 78-84, doi:10.1016/s0166-2236(96)10069-2 (1997).

45 Suzuki, H. *et al.* Involvement of estrogen receptor β in maintenance of serotonergic neurons of the dorsal raphe. *Mol Psychiatry* **18**, 674-680, doi:10.1038/mp.2012.62 (2013).

46 Bowman, G. L. *et al.* Blood-brain barrier breakdown, neuroinflammation, and cognitive decline in older adults. *Alzheimers Dement* **14**, 1640-1650, doi:10.1016/j.jalz.2018.06.2857 (2018).

47 Sandoval, K. E. & Witt, K. A. Age and 17beta-estradiol effects on blood-brain barrier tight junction and estrogen receptor proteins in ovariectomized rats. *Microvasc Res* **81**, 198-205, doi:10.1016/j.mvr.2010.12.007 (2011).

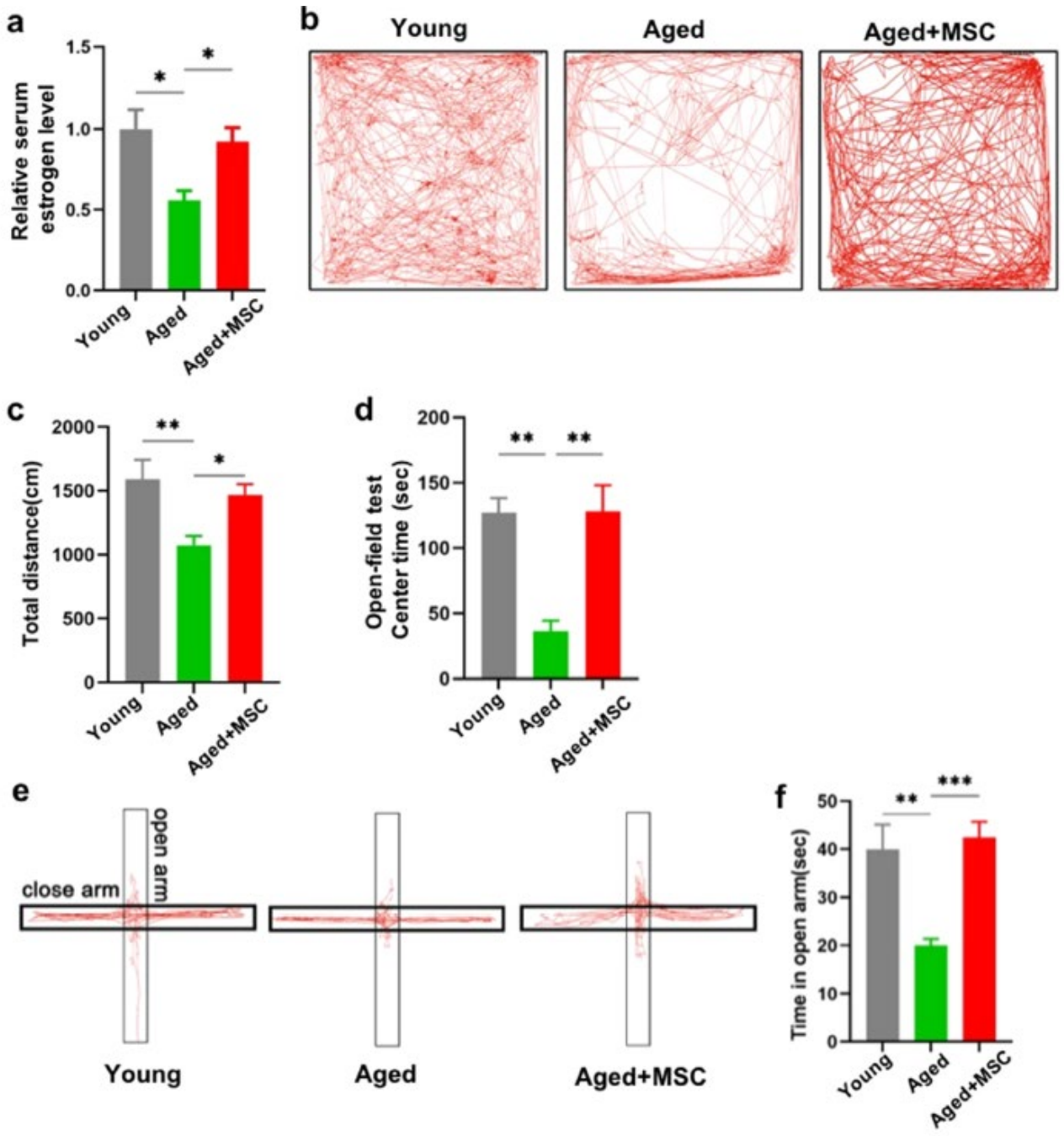

Fig. 1. MSC treatment alleviated anxiety-like behavior in aged mice. Relative serum estrogen level (a, n = 3–4) in young mice (n = 3), aged mice (n = 4) and aged mice treated with MSCs (n = 3), Open-field test performance (b), total distance traveled (c) and percent time spent in the center of the open field (d), as well as performance in the elevated-plus maze (e, n = 5–6) and total time spent in open arms (f) in young mice (n = 5), aged mice (n = 6) and aged mice treated with MSCs (n = 6). Results are presented as mean ± SEM, and analyzed using one-way ANOVA with Tukey post hoc tests. * $P < 0.05$, ** $P < 0.01$, *** $P < 0.001$.

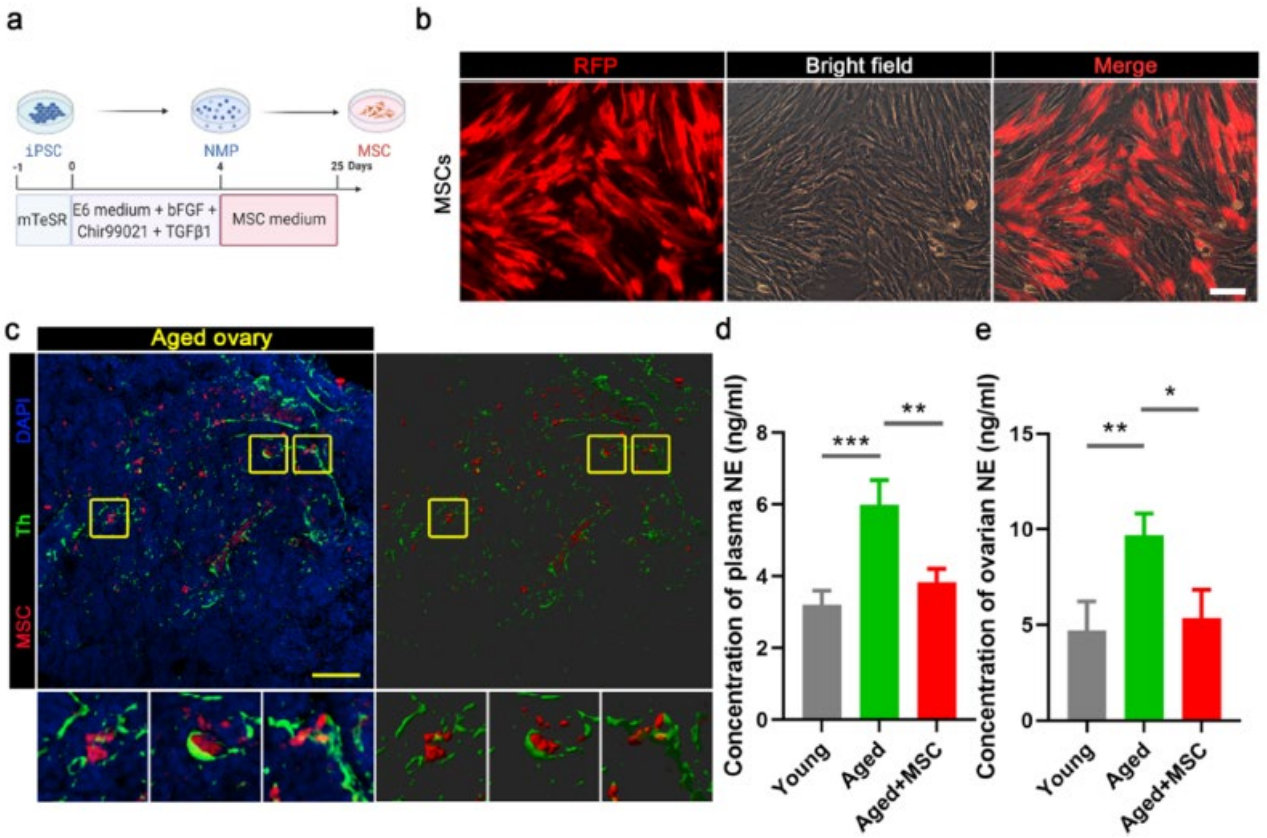

Fig. 2. iPSC-derived MSCs migrated to the ovaries and inhibited norepinephrine release from the sympathetic nerves. Schematic diagram of iPSC-derived MSCs (a). iPSC-derived MSCs were transduced with tdTomato lentivirus for tracing (Scale bar = 100 μm, b). Representative images of injected tdTomato-positive MSCs located close to ovarian sympathetic nerve stained with tyrosine hydroxylase (Th) in green (Scale bar = 50 μm, c). Plasma norepinephrine (NE) concentration in young mice (n = 4), aged mice (n = 4) and aged mice treated with MSCs (n = 3) (d). Ovarian NE concentration in young mice (n = 5), aged mice (n = 3), and aged mice treated with MSCs (n = 3) (e). Results are presented as mean ± SEM, and analyzed by one-way ANOVA with Tukey post hoc tests. * $P < 0.05$.

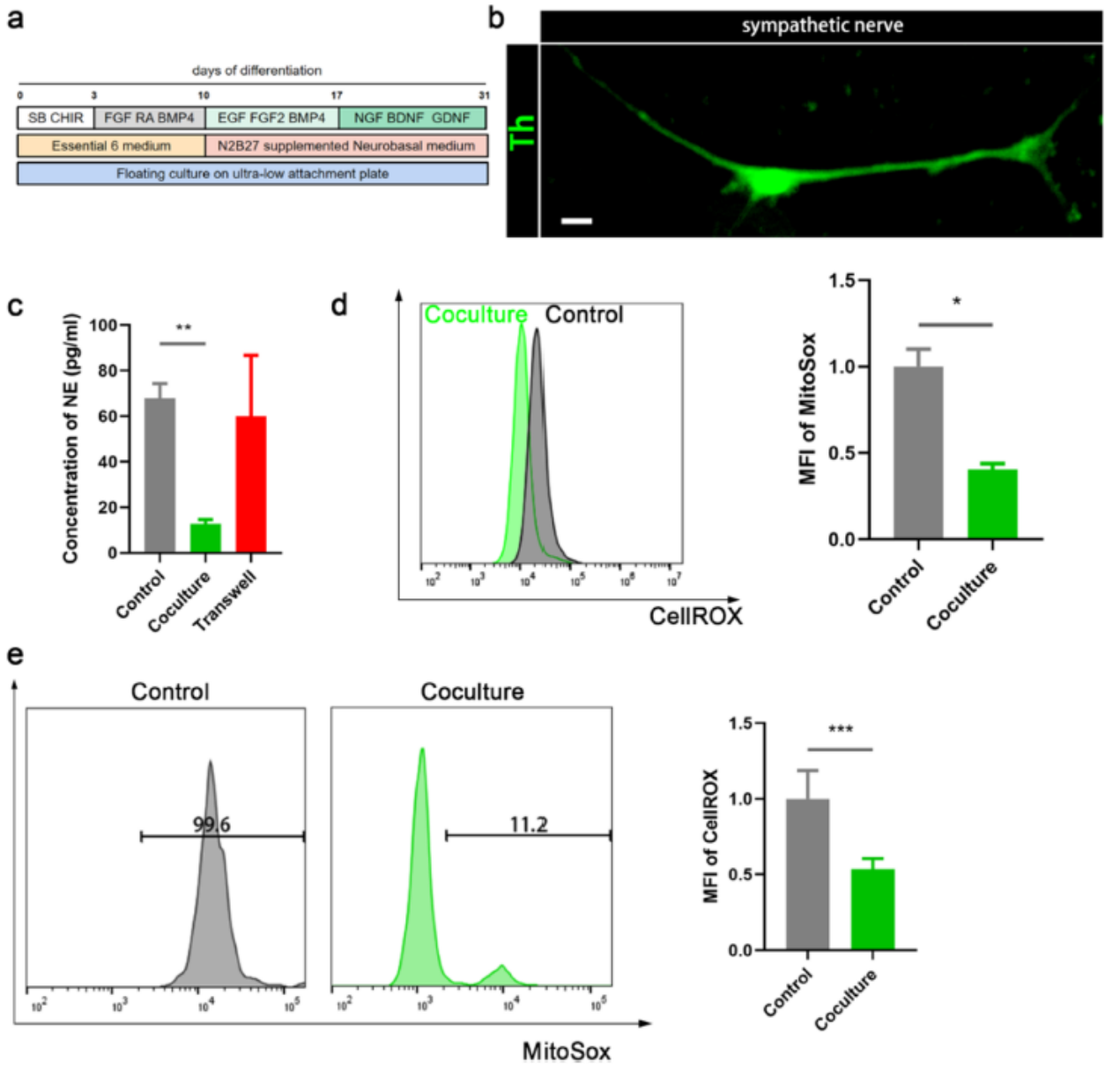

Fig. 3. MSCs inhibited norepinephrine secretion from sympathetic neurons in vitro. Schematic diagram of iPSC-derived sympathetic neuron (iPSCs-SNs) (a). Tyrosine hydroxylase (Th, green) staining in iPSC-derived sympathetic nerve (Scale bar = 100 ìm, b). Norepinephrine (NE) concentrations in the culture medium of sympathetic nerve alone (Control), direct co-culture (Coculture) and Transwell co-culture of MSCs and sympathetic neurons (n = 3, c). Whole cell (d) and mitochondrial (e) ROS levels reflected by flowcytometry relative mean fluorescence intensity (MFI) of CellROX staining in single-cultured iPSCs-SNs (Control) and direct cocultured (Coculture) iPSC-SNs and MSCs (n = 3). The results are presented as mean ± SEM. The data were analyzed using one-way ANOVA with Tukey post hoc tests (c), or unpaired student's t test (d and e). * $P < 0.05$, *** $P < 0.001$.

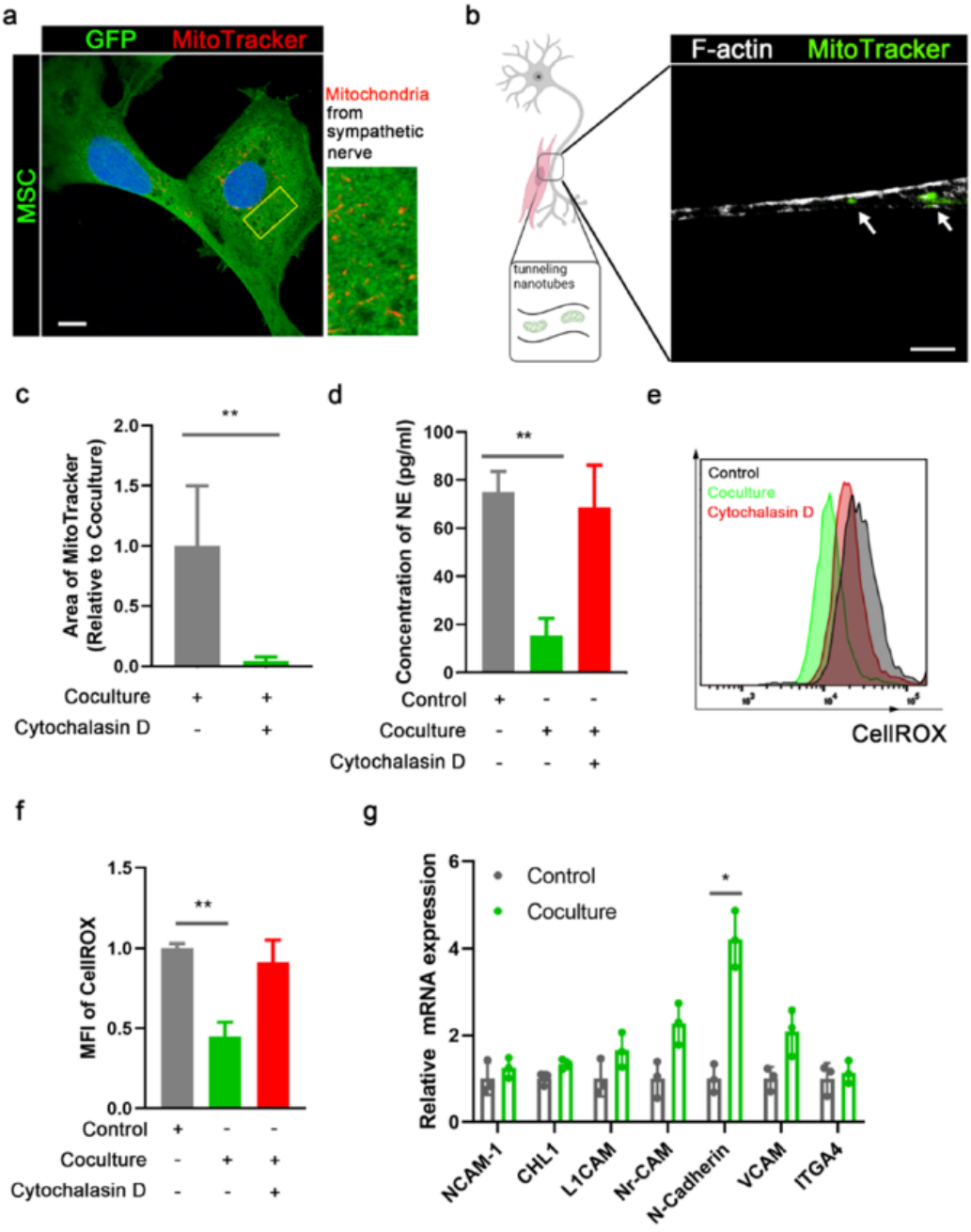

Fig. 4. Mitochondria transfer between sympathetic nerves and MSCs to suppress oxidative stress. Representative images showing that mitochondria from iPSC-SNs (MitoTracker, red) internalized in adjacent MSCs (GFP, green) (Scale bar = 10 μm, a). Representative image shows the presence of tunneling nanotubes (TNTs) (F-actin, grey) containing mitochondria (MitoTracker, green) (arrow) in the co-culture system (Scale bar = 5 μm, b). Areas of positive MitoTracker staining in co-cultured MSCs and iPSC-SNs, with and without Cytochalasin D (n = 3, c). Norepinephrine (NE) concentration in the culture medium of iPSC-SNs cultured alone (Control) or with MSCs (Coculture), with and without Cytochalasin D (n = 3, d). ROS levels reflected by fluorescence intensity (MFI) of CellROX staining (n = 3, e, f). mRNA expression of adhesion molecules in iPSC-SNs cultured alone (Control) or with MSCs (Co-culture) (n = 3, g). The results are presented as mean ± SEM and analyzed using one-way ANOVA with Tukey post hoc tests (d, f) or unpaired student's t test (c, g). ** $P < 0.01$.

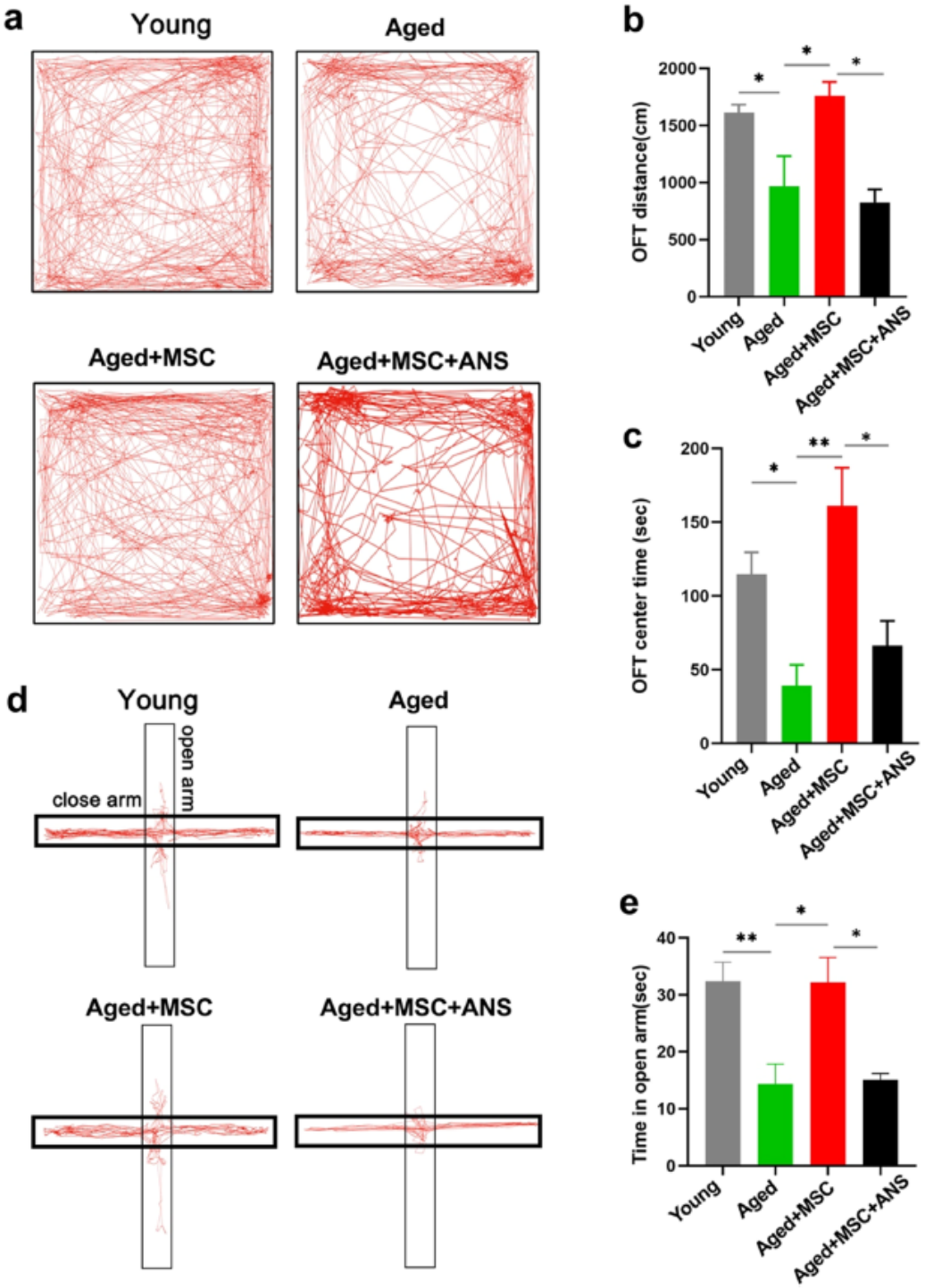

Fig. 5. Anastrozole (ANS) suppressed the therapeutic effects of MSCs. Activities in the Open-field test (OFT) for young mice (n = 7), aged mice (n = 5), aged mice treated with MSCs (Aged+MSC, n = 5), and aged mice treated with MSCs and anastrozole (Aged+MSC+ANS, n = 4) (a), total distance traveled (b), and time spent in the center (c). Activities in the elevated plus maze for young mice (n = 7), aged mice (n = 5), aged mice treated with MSCs (Aged+MSC, n = 5), and aged mice treated with MSCs and anastrozole (Aged+MSC+ANS, n = 4) (d), total time spent in open arms (e). The results are presented as mean ± SEM, and analyzed using one-way ANOVA with Tukey post hoc tests. *P < 0.05, * *P < 0.01.

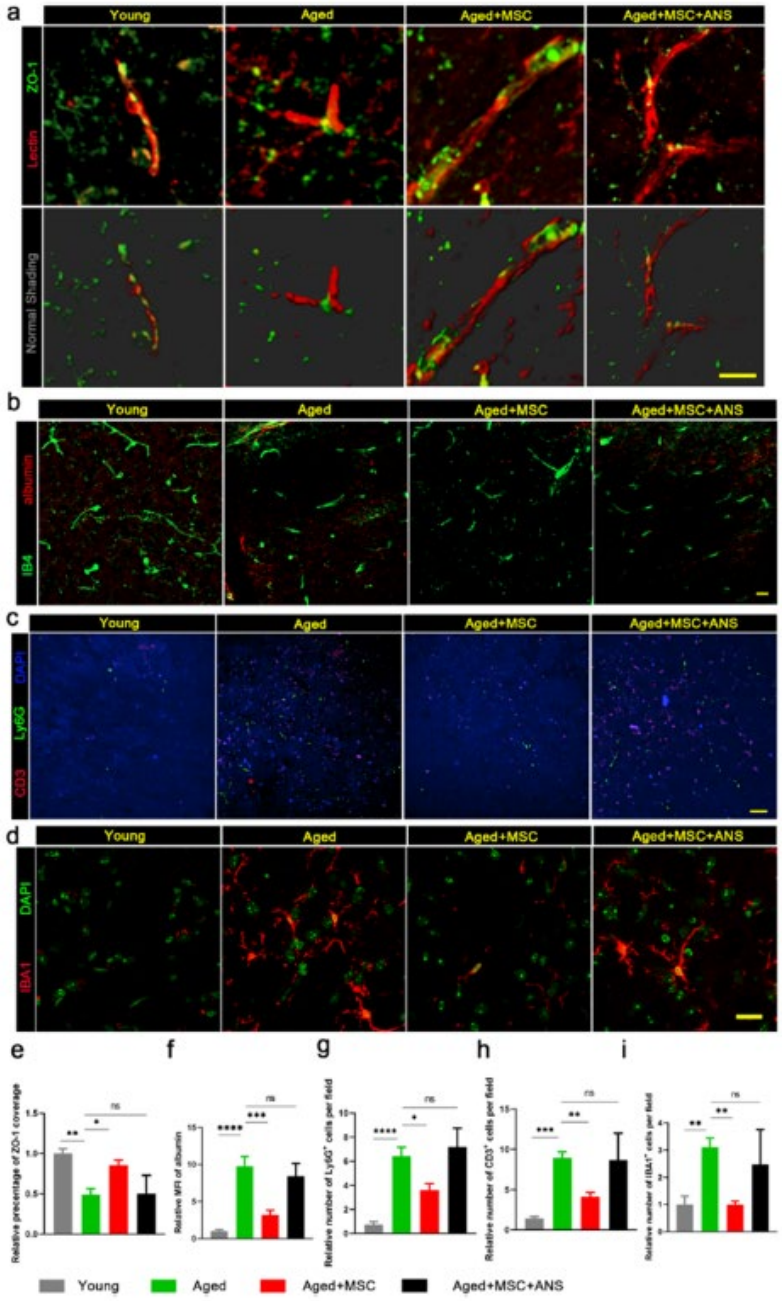

Fig. 6. MSC treatment improved BBB integrity and reduced neuroinflammation in aged mice. Representative images of tight junction protein ZO-1 (green) and lectin (red) co-staining (Scale bar = 20 μm), a), albumin (red) leakage from vessels (green) (Scale bar = 20 μm), b), Ly6g+ (green) or CD3+ (red) inflammatory immune cell infiltration (Scale bar = 50 μm), c) and IBA1+ microglial cells (red) (Scale bar = 20 μm), d) in the brains of young mice (n = 4), aged mice (n = 5), aged mice treated with MSCs (Aged+MSC, n = 5), and aged mice treated with MSCs and anastrozole (Aged+MSC+ANS, n = 4). Relative percentage of IB4 positive area associated with ZO-1 positive area (e); Relative mean fluorescence intensity (MFI) of albumin outside blood vessel (f); The relative number of Ly6g+ (g) or CD3+ cells (h), and IBA1+ cells per field (i). The results are presented as mean ± SEM, and analyzed using one-way ANOVA with Tukey post hoc tests. * $P < 0.05$, ** $P < 0.01$, *** $P < 0.001$, **** $P < 0.0001$.